THE TEMPERATURE SENSITIVITY OF A BISTABLE RAM

A Thesis

by

JANET KAY BROWN

Submitted to the Graduate College of
Texas A&M University
in partial fulfillment of the requirement for the degree of

MASTER OF SCIENCE

May 1986

Major Subject: Electrical Engineering

THE TEMPERATURE SENSITIVITY OF A BISTABLE RAM

A Thesis

by

JANET KAY BROWN

Approved as to style and content by:

Noel R. Strader
(Chairman of Committee)

Thomas R. Fischer
(Member)

Daniel Colunga
(Member)

Karan Watson
(Member)

Jo W. Howze
(Head of Department)

May 1986

ABSTRACT

The Temperature Sensitivity of
A Bistable RAM. (May 1986)
Janet K. Brown, M.S., Texas A&M University
Chairman of Advisory Committee: Dr. Noel R. Strader

Lu's Modified Trapping Model is applied to the polycrystalline-silicon resistor of a new bistable RAM cell. The effect of temperature on the resistor is explored with respect to the operation of the RAM cell's refresh mechanism. A temperature range of $0 - 100°C$ is investigated. The results are analyzed as the grain size, doping concentration, and length of the resistor are varied. The author concludes that for the test geometries specified by Çilingiroğlu, the creator of the bistable RAM, the RAM cell will fail to operate correctly over a temperature range of $0 - 100°C$. An optimization procedure is suggested to adjust the original parameters of the cell so that an operating temperature range $0 - 100°C$ may be achieved.

To my parents

TABLE OF CONTENTS

TABLE OF CONTENTS (Continued)

LIST OF TABLES

LIST OF FIGURES

CHAPTER 1

INTRODUCTION

The search for small, dense memories has led to the dynamic RAM cell which is comprised of one transistor and one capacitor. Unfortunately the refresh circuitry associated with dynamic RAM's is complex, often making them unsuitable for circuits integrating memory and logic. Static RAM is the current solution to this problem.

In [1-4] Çilingiroğlu has proposed an alternative to static RAM he calls the bistable RAM. This cell employs a charge pump to refresh the dynamically stored information and thus simultaneously avoids the large cell size of a static RAM while eliminating the complex refresh circuitry needed with the dynamic RAM.

Because of the refresh mechanism used the cell is sensitive to temperature and may fail to operate at temperatures extremes. It is the purpose of this research to specify the polysilicon resistor to be used in the cell so that the cell operates for temperatures between $0 - 100°C$.

So that the reader may fully appreciate the problem a review of the literature will be given. First the charge pump will be explained, and then the physics of the bistable cell will be analyzed. The modified trapping model which describes the behavior of the polysilicon resistor will be discussed in Chapter 3. In Chapter 4 the resistor specifications will be given, and Chapter 5 will present an analysis of the results and some conclusions.

Journal model is *IEEE Jounal of Solid-State Circuits.*

CHAPTER II

LITERATURE REVIEW

A. CHARGE PUMPING

Brugler and Jespers in [5] provide a basic explanation of charge pumping. A brief summary of that explanation follows.

Consider Figure 1. Before the gate pulse is applied, $V_g = V_{rb}$ and I_b is positive and equal to the reverse bias leakage current of the transistor. When V_g falls to V_{rp}, Figure 2, the n region under the gate is temporarily driven into deep depletion and the potential barrier between the n and p regions is lowered. Holes from the p regions rush under the gate of the transistor to restore equilibrium. When the pulse is removed V_g returns to V_{rb}. As V_g rises the misplaced charge under the gate attempts to return to the p regions. When $V_g = V_{rb}$, where $V_{rb} > V_{fb}$, any charge that failed to reach the p regions recombines in the substrate (Figure 3). V_{fb} is the flat-band voltage. This charge results in the pumping current I_p. The trapped charge density, Q_{trap}, per gate pulse is

$$Q_{trap} = \alpha Q_{free} + qN_{st} \tag{1}$$

where Q_{free} is the free charge hole density in the inversion layer (cm^{-2}), α is the fraction of free carriers which recombine in the bulk and N_{st} is the total fast surface-state density (cm^{-2}) which contributes to the effect.

When $V_g > V_s + V_t$, where V_s is the voltage applied to the p regions and V_t the threshold voltage, the surface is depleted and $Q_{free} \sim 0$. When $V_g < V_s + V_t$ the surface is in strong inversion and

$$Q_{free} = -C_{ox}(V_g - V_s - V_t) \tag{2}$$

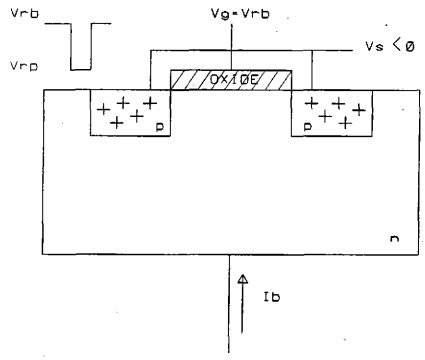

Fig. 1 The charge pump before the pulse is applied.

where C_{ox} is the oxide capacitance per unit area. Therefore the pumping current is given by

$$I_p = A_g f(-\alpha C_{ox}(V_g - V_s - V_t) + qN_{st}) \tag{3}$$

where A_y is the area of the gate and f is the pulse repetition frequency. This equation describes a phenomenon where during each gate pulse a quantity of charge is measured out under the gate and then pumped into the substrate.

The first term in (3) considers the effect of device geometry on I_p and is labeled

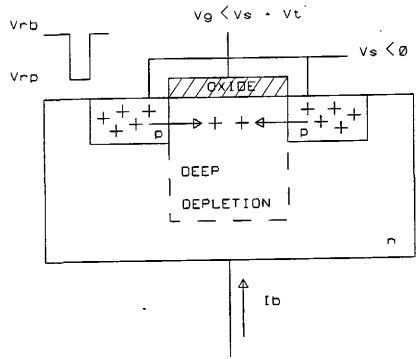

Fig. 2 The charge pump for $V_g < V_s + V_t$.

the "geometric component" by Brugler and Jespers. The polysilicon gate of the transistor and the n type substrate can be modeled as the parallel plates of a capacitor which are separated by a dielectric. When a gate pulse is applied holes are stored on the lower plate of this capacitor. These holes are free mobile carriers. For a slowly varying gate voltage the holes will have time to reach the junction before the inversion layer is removed. If V_g rises quickly more of the holes will fail to reach the junction, recombine in the bulk, and α will increase.

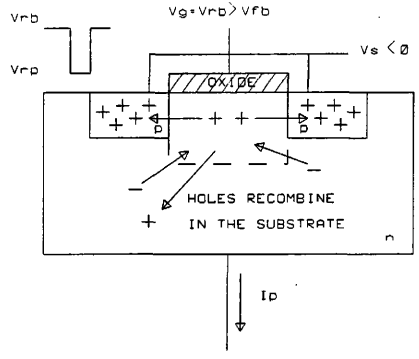

Fig. 3 The charge pump for $V_R = V_{rb}$.

The second term, "the surface-state component," explains the relationship between the pumping current and the surface-state density. Charge trapped in the surface states under the gate is always lost when the inversion layer is removed. To a first order approximation the surface-state density is given by

$$N_{st} = N_t(\phi_0 - \phi_s) \tag{4}$$

where N_t is the trap density, ϕ_0 the surface potential with zero gate voltage, and ϕ_s the surface-state potential with a negative gate voltage.

Therefore if the gate voltage is varied slowly, α will be small, and the amount of pumped charge can be controlled by altering the trap density, a processing step, or by controlling the surface potential.

B. THE PHYSICS OF THE BISTABLE RAM CELL

The material contained in this section was drawn from [1-4,6]. The configuration of the bistable RAM cell under consideration is shown in Figure 4. Figure 5 is a simpler drawing of the cell. Other configurations may be found in [1-3]. A pmos process is assumed although the results of this research may be applied to nmos. The storage gate potential is fixed at V_{rp} and the doping profiles beneath the pumping gate and storage gate are identical.

When a constant negative dc voltage is applied to the storage gate a potential well, the storage well, is formed. The storage well is accessed via the wordline transistor. Two states may then be defined: the full state when the storage well is full of holes. and the empty state when the storage well is empty.

When the well is in the empty state, holes from the substrate will leak into the well gradually filling the well. Therefore, a refresh mechanism must be supplied that will maintain the empty state. The refresh mechanism employed is Brugler and Jespers' charge pump.

First consider the empty state. When $V_g = V_{rp}$ the depth of the pump well and the storage well will be equal. When the refresh signal, V_r, returns to V_{rb}, V_g will begin to rise. The rate at which V_g rises is determined by the value of R and the capacitance of the pumping gate. Because the well is empty, the surface is deeply depleted, the gate capacitance is small, and thus V_g rises quickly. V_{gx} is the pump gate voltage for which the surface enters weak accumulation. When $V_g = V_{gx}$,

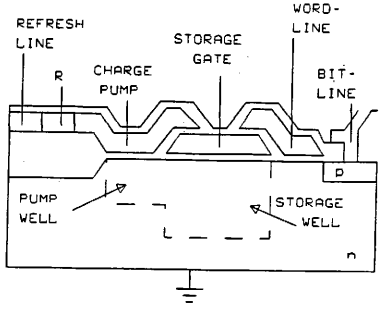

Fig. 4 Bistable RAM configuration.
Adapted from Çilingiroğlu [4].

electrons annihilate the holes trapped in the surface states and the pumping current begins to flow. Therefore during a refresh period in which V_g is allowed to rise to V_{gx} any charge trapped in the interface state traps will be pumped into the substrate. If the number of traps is greater than the number of holes leaking into the well during one refresh period, $T = T_B + T_P$, where T_P is the length of time $V_r = V_{rp}$, the peak level, and T_B the length of time $V_r = V_{rb}$, the base level, the empty state will be maintained.

Without the charge pump, the full state is stable. However if the charge pump is allowed to operate in the full state the pump will gradually empty the storage well. Therefore during the full state the charge pump must be disabled.

When the cell is in the full state and $V_g = V_{rp}$ the charge stored in the storage well will flow into the pump well until the pump and storage well surface potentials

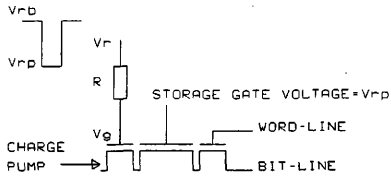

Fig. 5 The bistable RAM cell.
Adapted from Çilingiroğlu [4].

are equal. When V_r returns to V_{rb}, V_g will begin to rise. However because the pump well contains charge, the surface is not in deep depletion as in the empty state but rather in strong inversion. Therefore the gate capacitance will be large and the rate at which V_g rises to V_{gx} will be slow.

The full state and empty state waveforms are shown in Figure 6. For the cell to operate correctly, pumping charge in the empty state and inhibiting pumping in the full state, T_B must be greater than or equal to T_{empty} and less than T_{full}. So two constraints for proper operation have been identified: $I_p \geq I_L$, the pumping current must be greater than the leakage current, and $T_{empty} \leq T_B \leq T_{full}$.

Now let us analyze the cell for an arbitrary initial storage surface potential $\phi_{ss}(0)$. The following analysis follows [6]. From MOS theory the charge on the pump gate, Q_g, is given by

$$Q_g = A_p C_{ox}(V_g - \phi_{sp} - \phi_{ms}) \tag{5}$$

where A_p is the area of the pump gate. ϕ_{sp} the pump surface potential, and ϕ_{ms}

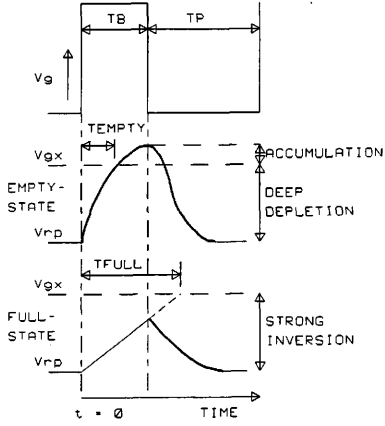

Fig. 6 Full and empty state waveforms.
Adapted from Çilingiroğlu [4].

the work function difference. Differentiating (5) with respect to time yields

$$I = A_p C_{ox} \frac{dV_g}{dt}(1 - \frac{d\phi_{sp}}{dV_g}). \tag{6}$$

The gate voltage may be related to the pump surface potential and the amount of

charge stored in the pump well, Q_p, by

$$V_g = V_{fb} + \phi_{sp} - V_o^{1/2}(-\phi_{sp})^{1/2} - Q_p/A_pC_{ox} \tag{7}$$

where V_{fb} is the flat-band voltage and V_o the body-factor. Similarly, the storage surface potential, ϕ_{ss}, may be related to the amount of charge in the storage well, Q_s, by

$$V_{rp} = V_{fb} + \phi_{ss} - V_o^{1/2}(-\phi_{ss})^{1/2} - Q_s/A_sC_{ox} \tag{8}$$

where A_s is the area of the storage gate.

Now consider Figure 7. When $V_g = V_{rp}$, charge stored in the storage well flows into the pump well until the storage and pump well surface potentials are equal. So, at $t = t_0$, $V_g = V_{rp}$ and $\phi_{sp}(0) = \phi_{ss}(0)$. At $t = t_{0+}$, V_r is switched to V_{rb} and ϕ_{sp} begins to rise. As ϕ_{sp} increases toward zero the charge stored in the pump well flows back into the storage well keeping the two surface potentials equal. While the pump well contains charge the capacitance of the well will be large and ϕ_{sp} will rise slowly. At some time, $t = t_1$ (Figure 8), all of the stored charge has been returned to the storage well, $\phi_{sp} = \phi_{ss}$, $Q_p = 0$, and $Q_s = Q_{total}$, where Q_{total} is the total amount of stored charge. During time $t_1 \leq t < t_2$ the storage surface potential remains approximately constant. The pump surface potential rises quickly because $Q_p = 0$ and the pump capacitance has been reduced. At $t = t_2$, $\phi_{sp} = \phi_f$ and $V_g = V_{gz}$. As V_g rises above V_{gz} the surface enters weak accumulation, electrons begin to annihilate the holes trapped in the fast surface states and the pumping current begins to flow.

So, two time intervals have been identified. During $t_0 \leq t < t_1$, $Q_p \neq 0$ and $\phi_{sp} = \phi_{ss}$. During $t_1 \leq t < t_2$, $Q_p = 0$. At $t = t_2$, $\phi_{sp} = \phi_f$ and charge pumping is initiated.

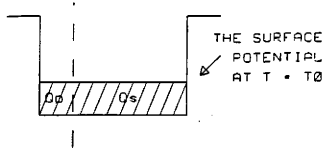

Fig. 7 Q_p and Q_s for an arbitrary $\varphi_s(0)$ at $t = t_0$.

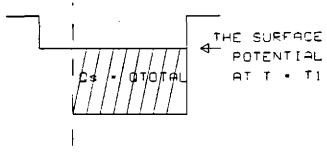

Fig. 8 Q_p and Q_s for an arbitrary $\varphi_s(0)$ at $t = t_1$.

Now consider the time interval $t_0 \leq t < t_1$. If the cell is not accessed the total stored charge, Q_{total}, remains constant. From (7) and (8) Q_{total}, is given by

$$Q_{total} = -C_{ox}(A_p V_g + A_s V_{rp}) + C_{ox}(A_p + A_s)(V_{fb} + \phi_{sp} - V_o^{1/2}(-\phi_{sp})^{1/2}). \quad (9)$$

Differentiating (9) with respect to time yields

$$0 = -A_p + (A_p + A_s)(\frac{d\phi_{sp}}{dV_g} + \frac{V_o^{1/2}}{2(-\phi_{sp})^{1/2}} \frac{d\phi_{sp}}{dV_g}). \quad (10)$$

Rearranging (10) produces

$$\frac{d\phi_{sp}}{dV_g} = \frac{A_p}{(A_p + A_s)(1 + V_o^{1/2}/2(-\phi_{sp})^{1/2})}. \quad (11)$$

Substituting (11) into (6) yields the differential equation

$$I = A_p C_{ox} \frac{dV_g}{dt}(1 - \frac{A_p}{(A_p + A_s)(1 + V_o^{1/2}/2(-\phi_{sp})^{1/2})}). \quad (12)$$

$\phi_{sp}(0)$ is close to $\phi_{sp}(t_1)$ and $V_o^{1/2}/2(-\phi_{sp})^{1/2}$ is small. Therefore ϕ_{sp} in (12) may be approximated by $\phi_{sp}(0)$ which yields

$$I = A_p C_{ox} \frac{dV_g}{dt}(1 - \frac{A_p}{(A_p + A_s)(1 + V_o^{1/2}/2(-\phi_{sp}(0))^{1/2})}). \quad (13)$$

If a full state is written while the pump well is in deep depletion both the pump well and the storage well will be filled with holes. When V_r is switched to V_{rb} the pump surface potential will begin to rise and charge will spill into the substrate. This charge, unlike the charge which leaks into the well during the empty state, did not originate in the substrate and therefore may flood the surrounding cells and destroy information. So, it is necessary to control the amount of charge written to a cell.

To prevent spillage, the storage well surface potential must never exceed ϕ_f, the surface potential at which accumulation begins. Thus if a small safety margin is employed ϕ_{ss} must remain $\leq 2\phi_f$. ϕ_{ss} reaches a maximum at $t = t_1$. So at $t = t_1$, letting $\phi_{ss}(max) = 2\phi_f$, yields

$$Q_{total}(max) = -A_s C_{ox}\left\{V_{rp} - V_{fb} - 2\phi_f + V_o^{1/2}(-2\phi_f)^{1/2}\right\} \tag{14}$$

from (8) where $Q_s = Q_{total} = Q_{total}(max)$.

At $t = t_0$, $V_g = V_{rp}$, $\phi_{sp}(0) = \phi_{ss}(0)$ and using (9)

$$Q_{total} = C_{ox}(A_p + A_s)\left\{-V_{rp} + V_{fb} + \phi_{sp}(0) - V_o^{1/2}(-\phi_{sp}(0))^{1/2}\right\}. \tag{15}$$

The maximum value of $\phi_{sp}(0)$ can then be found by substituting $Q_{total}(max)$ in (14) for Q_{total} in (15). Doing this and solving yields

$$\phi_{sp}(0)(max) = -\frac{1}{4}\left\{-V_o^{1/2} + \sqrt{V_o - 4\left(\frac{Q_{total}(max)}{C_{ox}(A_p + A_s)} + V_{rp} - V_{fb}\right)}\right\}^2. \tag{16}$$

So, when a full state is written, charge will be allowed to fill the cell until $\phi_{ss} = \phi_{sp}(0)(max)$. Then if the pump well is in deep depletion when a full state is written (e.g. $V_g = V_{rp}$), $\phi_{ss}(t_1) = \phi_{sp}(t_1) = 2\phi_f$ and spillage will be prevented. Because refreshing is asynchronous with respect to read/write operations, a full state could be written while $V_g \geq V_{gx}$. If this happened only the storage well would be filled, the total amount of stored charge would be a minimum, $\phi_{ss}(t_1) = \phi_{sp}(0)(max)$ and from (8)

$$Q_{total}(min) = -A_s C_{ox}\left\{V_{rp} - V_{fb} - \phi_{sp}(0)(max) + V_o^{1/2}(-\phi_{sp}(0)(max))^{1/2}\right\}. \tag{17}$$

Then when V_g returned to V_{rp}, $\phi_{sp}(0)(min)$ would be

$$\phi_{sp}(0)(min) = -\frac{1}{4}\left\{-V_o^{1/2} + \sqrt{V_o - 4\left(\frac{Q_{total}(min)}{C_{ox}(A_p + A_s)} + V_{rp} - V_{fb}\right)}\right\}^2. \tag{18}$$

Recall that (12) was approximated by (13) by letting $\phi_{sp} = \phi_{sp}(0)$ since the total range of values for ϕ_{sp} was small. The use of $\phi_{sp}(0)(min)$ in (13) will produce a conservative (the shortest) estimate of the time from t_0 to t_1 when the cell is in the full state.

Now consider the time interval $t_1 \leq t < t_2$. In this interval $d\phi_{sp}/dV_g$ is approximately constant. Letting $d\phi_{sp}/dV_g = H$ gives from (6)

$$I = A_p C_{ox}(1 - H)\frac{dV_g}{dt}. \tag{19}$$

So four governing equations have now been identified:

$$I_p \geq I_L, \tag{20}$$

$$T_{empty} \leq T_B \leq T_{full}, \tag{21}$$

$$I = A_p C_{ox}\frac{dV_g}{dt}\left(1 - \frac{A_p}{(A_p + A_s)(1 + V_o^{1/2}/2(-\phi_{sp}(0))^{1/2})}\right) \tag{22}$$

for $t_0 \leq t < t_1$ and

$$I = A_p C_{ox}(1 \quad H)\frac{dV_g}{dt} \tag{23}$$

for $t_1 \leq t < t_2$.

CHAPTER III

THE MODIFIED TRAPPING MODEL

In [7] Lu proposes two models for polysilicon passive devices, the modified trapping model which considers only thermionic emission and which clarifies and extends the work of Seto [8], Baccarani et. al.[9], Tarng [10] and others, and the TE+TFE+TFES model which includes the combined effects of thermionic emission, thermionic field emission, and scattering at the grain boundaries. The modified trapping model was used in this research instead of the TE+TFE+TFES model for the two reasons outlined below.

Thermionic emission (TE) is based on the classical premise that only carriers with energy greater than qV_B can surmount a potential barrier of height V_B. This idea has been modified by quantum mechanics, where carriers with energy $< qV_B$ can tunnel through potential barriers and where some carriers with energy $> qV_B$ will be reflected. This quantum mechanical transport mechanism is thermionic field emission (TFE). Lu in [7] calculates the ratio of TFE current to TE current. This ratio is plotted against temperature in Figure 9. For temperatures $> 0°C$ this ratio is < 1 and TE is the dominate transport mechanism.

The second reason the modified trapping model was chosen, was that although the TE+TFE+TFES model is more accurate, especially at low temperatures, it requires that four physical parameters e_t, Q_t, χ and δ be known. e_t is the trapping state energy of the grain boundary traps, Q_t is the grain boundary trapping state density, χ is the grain boundary potential barrier height above V_B, and δ is the grain boundary potential barrier width. The modified trapping model requires a knowledge of only e_t and Q_t. Because the modified trapping model has been studied by others, approximate values for e_t and Q_t can be found in the literature. Seto

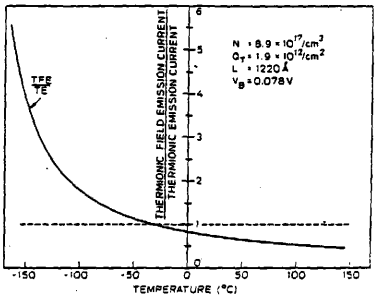

Fig. 9 TFE/TE current ratio as a function of temperature. From Lu [7].

[8] gives $Q_t \sim 3.34 \times 10^{12}$ and $e_t \sim -.18$ for a grain size $L = 230$Å. Lu's data, [7], yields $Q_t \sim 1.9 \times 10^{12}$ and $e_t \sim -.17$ for $L = 1220$Å. Values for χ and δ must either be obtained from only Lu's work or from actual measurements. Since such measurements were not available to the author, and since thermionic emission is still the dominate conduction process even at 0°C the modified trapping model was used.

The following development of the transport equation is drawn from [7].

Each grain (crystallite) is considered to be a rectangle of width L and cross-

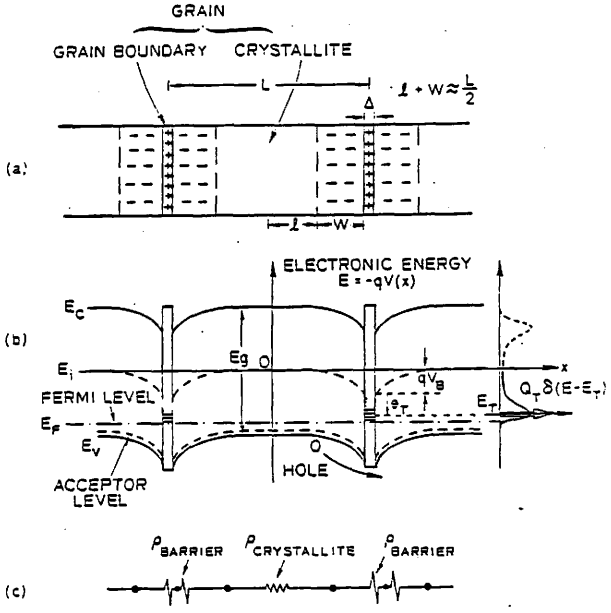

Fig. 10 Modified polysilicon trapping model.
From Lu [7].

sectional area A. Such a crystallite is shown in Figure 10a. One dimensional transport through the crystallite is assumed. The edge (boundary) of the crystallite has a random structure which leads to the formation of trapping states. However the center of the crystallite is composed of ordered atoms and may be considered single crystal material. When the polysilicon film is doped an impurity level is formed inside the crystallites, and impurity atoms are ionized to create majority mobile carriers. These carriers are trapped in the grain boundary trapping states, depleting the crystallite and forming a potential barrier at the grain boundary. The energy-band diagram is shown in Figure 10b (p. 16). E_i, the intrinsic Fermi level, is the zero reference. Using the depletion approximation and Poisson's equation the potential barrier height can be derived as

$$V_B = \frac{qNW^2}{2\epsilon} \tag{24}$$

where N is the doping concentration, W the depletion region width, and ϵ the permittivity of silicon.

There exists a doping concentration N^* at which all of the available traps have been filled. For $N < N^*$ the width of the depletion region extends throughout the crystallite and $2W = L$. For $N > N^*$, $2W < L$ and the crystallite is no longer completely depleted.

Lu calculates N^* by first finding the effective trapping state density Q_t^*, which is related to Q_t, the number of metallurgical traps per cm^2 by

$$Q_t^* = \frac{Q_t}{1 + 2\exp[(E_F - e_t + qV_B)/kT]} \tag{25}$$

where k is Boltzman's constant, T absolute temperature and E_F the Fermi level. So, when $N < N^*$ the Fermi level is pinned by the grain boundary trapping states.

At the center of the grain, the hole concentration $p(0)$ is given by

$$p(0) = ni \exp(-E_F/kT) \tag{26}$$

where ni is the intrinsic carrier concentration given as

$$ni = 2(\frac{2\pi kT}{h^2})^{3/2}(m_e^* m_h^*)^{3/4} \exp(-E_g/2kT) \tag{27}$$

where h is Planck's constant, m_h^* is the conductivity effective mass of holes, m_e^* the conductivity effective mass of electrons, and E_g the band gap energy of silicon.

When $N = N^*$ all available traps have been filled and $p(0) = N^*$. Therefore if Q_t^* is equated to the number of ionized dopants in the depletion region, $Q_t^* = N2W$, (25) and (26) can be combined to yield

$$N^* = \frac{Q_t}{L} - 2ni \exp(-e_t/kT) \exp(q^2 N^* L^2/8\epsilon kT) \tag{28}$$

which can be iteratively solved for N^*.

A. CALCULATING THE CURRENT DENSITY FOR $N < N^*$

The transport equation is

$$J_B = 2qp(0)(\frac{kT}{2\pi m_h^*})^{1/2} \exp(\frac{-qV_B}{kT}) \sinh(\frac{qV_{ba}}{2kT}) \tag{29}$$

where V_{ba} is the voltage which drops across a single barrier.

When $N < N^*$ each grain is totally depleted and V_{ba} equals V_a/N_g where V_a is the applied voltage and N_g is the number of grains. V_B can be found by substituting $W = L/2$ in (24). E_F can be found from (25) by equating Q_t^* and $2NW$, as

$$E_F = e_t - qV_B + kT \ln(1/2(\frac{Q_t}{LN} - 1)). \tag{30}$$

$p(0)$ can then be calculated using (26). Following this procedure J_B can be determined.

B. CALCULATING THE CURRENT DENSITY FOR $N > N^*$

When $N > N^*$ the crystallite contains both depleted and neutral regions. Dopant atoms in the neutral region are ionized to an impurity concentration N^+ given by

$$N^+ = \frac{N}{1 + 2\exp[(E_A - E_F)/kT]} \tag{31}$$

where E_A is the acceptor impurity level. In the neutral region $p(0) = N^+$ so equating (31) and (26) yields

$$ni\exp(-E_F/kT) = \frac{N}{1 + 2\exp[(E_A - E_F)/kT]} \tag{32}$$

which can be iteratively solved for E_F and $p(0)$. W can be then be found from (25) to be

$$W = \frac{Q_t}{2N[1 + 2(ni/N^+)\exp(-e_t/kT)\exp(q^2NW^2/2\epsilon kT)]}. \tag{33}$$

Once W is known V_B can also be determined.

Now refer to Figure 10c (p. 16). Since the resistivity of single crystal silicon is much smaller than the barrier resistivity, it can be neglected when W is large. But as N increases above N^*, W becomes small and the crystallite resistivity, ρ_c, becomes significant. ρ_c may be approximated by

$$\rho_c = \frac{1}{q\mu_h p(0)} \tag{34}$$

where μ_h is the hole mobility [11].

At 300°K, μ_h may be approximated by

$$\mu_h = 47.7 + (495.0 - 47.7)/(1 + (\frac{p(0)}{6.3 \times 10^{16}})^{.76}) \tag{35}$$

which is temperature independent [12]. Since ρ_c becomes significant only for large doping concentrations and since the temperature sensitivity of μ_h decreases as N increases, the error introduced by (35) will be small.

In [7] the voltage which drops across the crystallite bulk, V_c, is given as

$$V_c = J_c(L - 2W)\rho_c. \tag{36}$$

Since $V_c + V_{ba} = V_a/N_g$ and since $J_c = J_B$, (29) and (36) can be simultaneously solved with an iterative numerical procedure.

C. THE SENSITIVITY OF RESISTIVITY TO DOPING CONCENTRATION

First let us analyze the behavior of ρ, the resistivity, as N is increased to N^*. $p(0)$ will increase as N increases because the Fermi level moves toward the valence band as the boundary layer traps become filled. Since W is a constant, $V_B \propto N$. So, at a given temperature the transport equation will be dominated by two competing terms, $p(0)$ and V_B. $p(0)$ will tend to increase J_B as N increases and V_B, because it contributes to a negative exponential, will tend to decrease J_B. $p(0)$ wins the battle. Therefore the resistivity will gradually decrease as N increases toward N^*

Now let us examine how the TCR, the temperature coefficient of resistance, varies as the doping concentration increases above N^*. From (26), it can be seen that as the doping concentration increases and E_F moves toward the valence band, $p(0)$ will increase. Physically this means that since the boundary layer traps have been filled, any additional ionized carriers are free to conduct. From (33), it can be seen that the depletion region width decreases as N increases. The depletion width shrinks because the number of dopant atoms within the depleted region must remain equal to the number of available traps. Thus as the number of dopant atoms per cm^3 increases the deletion layer width must decrease. As W shrinks the potential barrier height will also fall. So whereas $p(0)$ and V_B fought against one another in the transport equation when $N < N^*$ they now work together to increase J_B and

reduce the resistivity rapidly. Therefore when $N < N^*$ the resistivity will decrease slowly as N increases and when $N > N^*$ the resistivity will decrease quickly.

CHAPTER IV

THE EFFECT OF TEMPERATURE

Chapter 2 introduced the physics of the bistable cell and Chapter 3 reviewed the modified trapping model. This chapter will first analyze the polysilicon resistor with respect to temperature and then will apply this analysis to the cell to discover the limiting constraints placed on the cell by temperature. These constraints together with the four governing equations will specify the resistor.

A. THE EFFECT OF TEMPERATURE ON THE RESISTOR

First reconsider (29), the transport equation. The following terms $p(0)$, $(kt/2\pi m_h^*)^{1/2}$, and $\exp(-qV_B/kT)$ increase as temperature increases. These terms overwhelm the sinh factor and produce a negative temperature coefficient of resistance (TCR).

At low doping concentrations. $N < N^*$, $|E_F|$ is small and p(0) is highly dependent on temperature. As N increases E_F increases and $p(0)$ eventually becomes only a weak function of temperature. V_B is temperature independent for $N < N^*$. However as N increases above N^*, V_B becomes a function of temperature, increasing at lower temperatures, and therefore contributes to a negative TCR. Since V_B decreases rapidly as the doping concentration increases above N^*, it's significance is reduced and $p(0)$, whose sensitivity to temperature is decreasing, remains the dominate factor. So, as the doping concentration increases the temperature sensitivity of the resistor will decrease.

B. THE EFFECT OF TEMPERATURE ON THE BISTABLE CELL

Reconsider (21), the second governing equation. The limiting constraint occurs

when T_{full} is a minimum and T_{empty} a maximum. Since the bit line is capable of totally emptying the cell, and since the charge pump can maintain the empty state, Q_p in the empty state is always ~ 0. Therefore, in the empty state, $\phi_{ss}(0) = \phi_{ss}(t_1)$ and (23) can be used to determine the time T_{empty}. T_{empty} is inversely proportional to I. So, over a temperature range of $0 - 100°C$, T_{empty} will be a maximum at 0°C.

The analysis of the full state is only slightly more complicated because both (22) and (23) must be used to calculate T_{full}. Eq. (22) should be used when $V_g \leq V_g(t_1)$ and (23) when $V_g \geq V_g(t_1)$. T_{full} will be the sum of the two times found. Because T_{full} is also inversely proportional to I, $T_{full}(min)$ ocurrs at 100°C.

$T_{full}(min) = T_{full}(100°C)$ and $T_{empty}(max) = T_{empty}(0°C)$. Therefore to satisfy (21), $T_{full}(100°C)$ must be greater than $T_{empty}(0°C)$. If the resistance varies too much from $0 - 100°C$, $T_{empty}(0°C)$ will exceed $T_{full}(100°C)$ and a suitable T_B will not exist. The resistance variation with temperature decreases as the doping concentration increases. So there is some minimum doping concentration that must be used to satisfy (21).

C. COMPUTER ANALYSIS

A computer program was written to determine the minimum doping concentration. The basic cell parameters used in the program were specified by Dr. Çilingiroğlu and are listed in Table I [6]. The main program, INT, integrates (22) and (23) as neccessary to find T_{full} and T_{empty} for a Boron doped resistor. The values of E_A, the impurity level of Boron, and E_g, the band gap energy were calculated using formulas found in [7]. The main program and the subroutines selected the full state model or the empty state model by simply testing the temperature. Since the resistor was tested for a range of $0 - 100°C$, the calculations were per-

formed for the full state when $T > 50°C$ and for the empty state when $T < 50°C$. Unless otherwise stated a state-of-the-art resistor was assumed, with characteristic dimensions $5\mu m \times 5\mu m \times .3\mu m$ [7]. For $L = 1220$Å, 420Å, and 230Å, $N_g = 42$, 117, and 218 grains respectively.

TABLE I.
BISTABLE RAM CELL PARAMETERS.
SPECIFIED BY ÇILINGIROĞLU [6].

V_{rb}	Refresh base voltage	0	volts
V_{rp}	Refresh peak voltage	-10	volts
t_{ox}	Oxide thickness	750	Å
A_s	Source gate area	120	μm^2
A_p	Pump gate area	24	μm^2
N_D	Substrate doping concentration	5×10^{15}	cm^{-3}
N_{st}	Surface-state density	10^{11}	cm^{-2}

Subroutine F2 calculates V_{gx}, H, $V_o^{1/2}$, and $\phi_{sp}(0)(min)$ and $V_g(t_1)(min)$ for the full state. These variables are independent of the doping concentration but dependent on temperature. H is found by incrementing V_g from $V_g(t_1)$ to V_{gx} and calculating ϕ_{sp} at each point. A least squares algorithm is applied to find the slope, $d\phi_{sp}/dV_g$, of the best fitting straight line. Since H is only approximately linear, the value of H in the full state will differ from the value of H in the empty state because $V_g(t_1)$ is different for each state. Figure 11 is a flowchart of this subroutine.

Subroutines G1 and G2 derive $p(0)$, V_B, and W for $N > N^*$ and $N < N^*$ respectively. Subroutine NST iteratively calculates N^* from (28). Figures 12 and 13 are flowcharts of G1 and G2. A flowchart of NST has not been included because of the simplicity of the subroutine.

The main program begins by calculating T_{empty} at $T = 0°C$ with NST,F2 and then either G1 or G2 depending on the doping concentration. After these calculations are completed all the parameters needed to find J_B in (29) will be

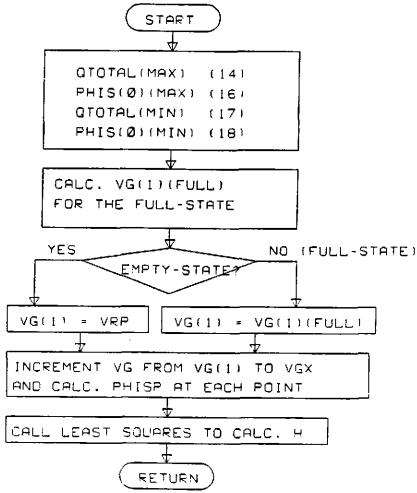

Fig. 11 Subroutine F2 flowchart. The numbers in parenthesis refer to equations in this document.

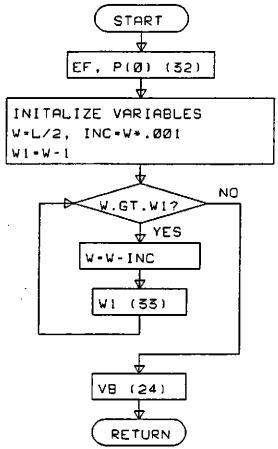

Fig. 12 Subroutine G1 flowchart.

known for a given V_g. Here the program calls QA05A/AD, a numeric integration system subroutine, which is capable of integrating a function. QA05A/AD requires that the user define a function which will return a derivative, in this case dt/dV_g, when it receives the independent variable, V_g, from the calling routine. The value of t returned by QA05A/AD is T_{empty}. The temperature is then changed to 100°C.

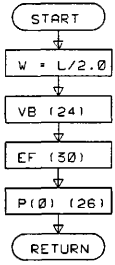

Fig. 13 Subroutine G2 flowchart.

and the above procedure is repeated resulting in T_{full}. Figure 14 is a flowchart of the main program.

The user defined function DER, which is called by QA05A/AD, is flowcharted in Figure 15 and considers the effect of bulk crystallite resistivity.

The main program is structured so that a number of different parameters can be varied. Appendix A contains a listing of the main program and each of the subroutines with the exception of QA05A/AD and the least squares algorithm.

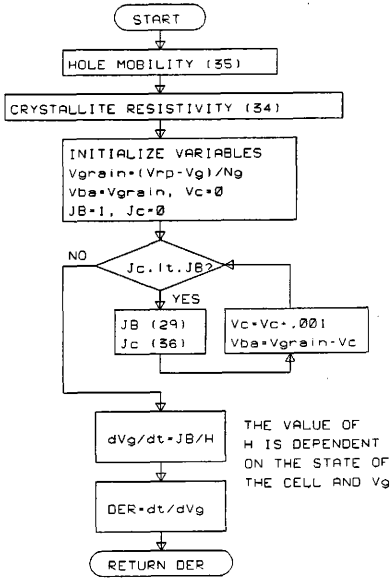

Fig. 14 Flowchart of Main program, INT.

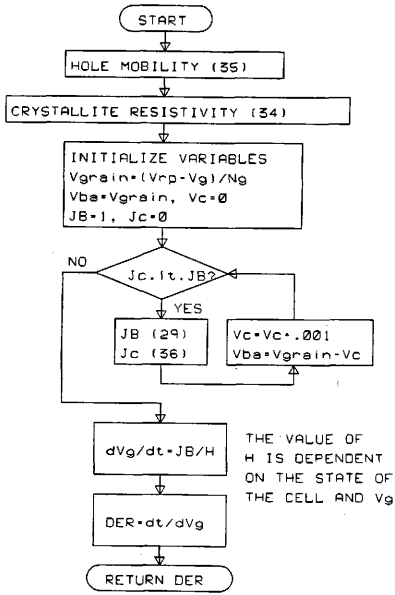

Fig. 15 Flowchart of user defined function, DER.

D. THE VARIATION OF TB_{safety} WITH DOPING CONCENTRATION

TB_{safety} is defined as the difference $T_{full}-T_{empty}$ and must be positive if (21) is to have a solution. Figure 16 is a graph of the output from a variation of INT which logarithmically increments the resistor doping concentration and records TB_{safety} at each point. Notice that, as predicted, the initially negative TB_{safety} steadily increases toward zero and then changes sign indicating that $T_{full} > T_{empty}$ and (21) has a solution. Note however that for $N \geq 10^{17.9}$ TB_{safety} begins to decrease slowly. The reason is that at such high doping concentrations the depletion region width is narrow and the bulk crystallite resistivity begins to contribute significantly to the total resistivity of the material. Since the effect of temperature on the mobility was neglected, the crystallite has a slightly negative TCR and thus TB_{safety} decreases slightly.

Figure 17 simply reiterates the concept just presented in a slightly different manner. Here INT has been adjusted so that TB_{safety} is calculated for successively larger temperature operating ranges. As the operating range is increased the sensitivity of the resistor to temperature causes the refresh mechanism to fail and TB_{safety} goes negative.

E. THE VARIATION OF THE MINIMUM ALLOWABLE DOPING CONCENTRATION WITH GRAIN SIZE

Table II lists N^* and the lowest value of N for which TB_{safety} is positive for $L = 1220$Å, 420Å, and 230Å. As the grain size decreases the disorder of the material increases and Q_t increases. This pushes N^* up, preserving the high resistivity and TCR at higher doping concentrations. Therefore the resistivity and the TCR will begin their rapid decent at progressively higher doping concentrations as the grain

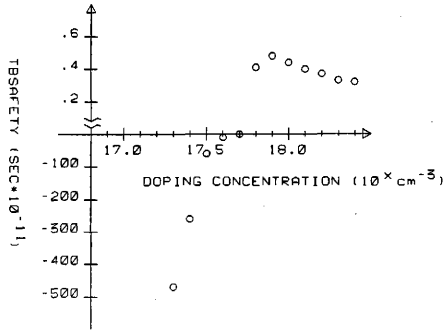

Fig. 16 TB_{safety} verses doping concentration. L = 1220Å.

size decreases. So as the grain size decreases, a higher doping concentration will be necessary to achieve the same insensitivity to temperature.

F. THE VARIATION OF TB_{safety} WITH THE NUMBER OF GRAINS

Table III lists the value of TB_{safety} at two doping concentrations for $L = 1220$Å and N_g = 42, 52, 62, 72 and 82 grains. In Table III $|TB_{safety}|$ increases as N_g increases. This can be explained as follows.

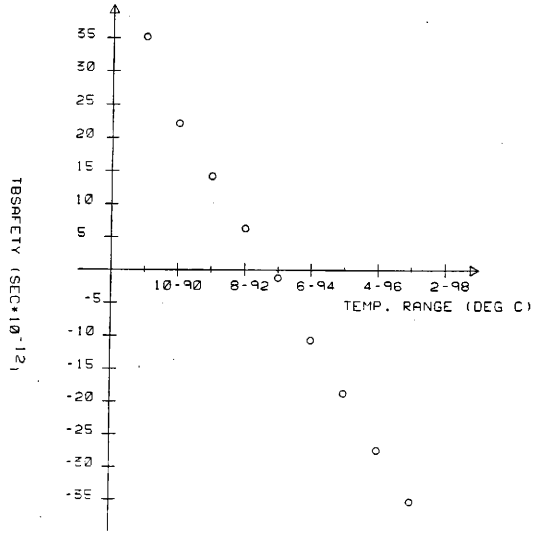

Fig. 17 TB_{safety} verses temperature range.

TABLE II.
THE MINIMUM ALLOWABLE DOPING CONCENTRATIONS FOR THREE GRAIN SIZES

$\sim N^*$ (cm^{-3})	N (cm^{-3})	L (Å)	Q_t (cm^{-2})	N_g
1.0×10^{17}	$10^{17.8}$	1220	1.90×10^{12}	42
6.7×10^{17}	$10^{18.2}$	420	3.00×10^{12}	119
1.4×10^{18}	$10^{18.4}$	230	3.34×10^{12}	217

TABLE III.
TB_{safety} FOR TWO DOPING CONCENTRATIONS AND SEVERAL VALUES OF N_G

TB_{safety} (sec)	N_g	N (cm^{-3})
-6.7233×10^{-11}	42	$10^{17.7}$
-9.5220×10^{-11}	52	$10^{17.7}$
-1.2866×10^{-10}	62	$10^{17.7}$
-1.5982×10^{-10}	72	$10^{17.7}$
-1.9733×10^{-10}	82	$10^{17.7}$
$+4.1030 \times 10^{-11}$	42	$10^{17.8}$
$+5.0175 \times 10^{-11}$	52	$10^{17.8}$
$+6.0363 \times 10^{-11}$	62	$10^{17.8}$
$+6.9206 \times 10^{-11}$	72	$10^{17.8}$
$+7.7913 \times 10^{-11}$	82	$10^{17.8}$

The current through the resistor is given by

$$I = I_s \sinh(\frac{qV_{ba}}{2kT}) \tag{37}$$

where I_s is the pre-sinh factor in (29) multiplied by the cross-sectional area A. I_s is independent of N_g. Letting $V_{ba} = (V_{rp} - V_g)/N_g - V_c$ and approximating the sinh by an exponential yields

$$I = I_s \exp(\frac{-qV_c}{2kT}) \exp(\frac{qV_{rp}}{2kTN_g}) \exp(\frac{-qV_g}{2kTN_g}). \tag{38}$$

Substituting (38) in (22) or (23) yields

$$I = I_s \exp(\frac{-qV_c}{2kT}) \exp(\frac{qV_{rp}}{2kTN_g}) \exp(\frac{-qV_g}{2kTN_g}) = A_p C_{ox}(1 - H^*) \frac{dV_g}{dt} \tag{39}$$

where H^* is the appropriate expression for $d\varphi_{sp}/dV_g$. Solving (39) yields

$$\Delta t = \frac{2kTN_gA_pC_{ox}(1-H^*)}{I_sq}\exp(\frac{qV_c}{2kT})\exp(\frac{-qV_a}{2kTN_g}). \quad (40)$$

Thus

$$TB_{safety} = N_g[K_1\exp(\frac{qV_c}{2kT_1})\exp(\frac{-qV_a}{2kN_gT_1}) - K_2\exp(\frac{qV_c}{2kT_2})\exp(\frac{-qV_a}{2kN_gT_2})] \quad (41)$$

where K_I is

$$K_I = \frac{2kT_IA_pC_{ox}(1-H^*)}{I_sq} \quad (42)$$

for $T_1 = 373°\text{K}$ and $T_2 = 273°\text{K}$ and $I = 1,2$ respectively.

For certain low doping concentrations where $V_c \ll V_a/N_g$, the exponential terms containing V_c do not contribute to the value of TB_{safety} and $|TB_{safety}|$ increases with N_g. As N increases the width of the depletion region decreases and V_c increases. Recall that $J_B = J_c$. So, from (29) and (36)

$$J_s\sinh(\frac{qV_{ba}}{2kT}) = V_c(L-2W)\rho_c. \quad (43)$$

Since $V_{ba} + V_c = V_a/N_g$, as N_g increases V_c and V_{ba} will decrease. Eq. (43) reveals that V_c will decrease more than V_{ba}. This will cause the difference between the two exponential terms containing V_c to decrease and thus the sign of TB_{safety} may change as N_g is increased. Finally as N increases still further so that $V_c \sim V_a/N_g$, the exponential terms in (41) cancel and $TB_{safety} \sim N_g(K_1 - K_2)$.

G. THE EFFECT OF TEMPERATURE ON T_B

In Chapter 2, four governing equations were presented. Three of these have been used to analyze the performance of the resistor. The remaining equation, (20),

states that $I_p \geq I_L$. Assuming that J_L, the worst case leakage current density is $\sim 2\text{amp/cm}^2$, $I_L = 2(A_p + A_s)$. If α is small I_p can be found from (3) to be

$$I_p = qA_p f N_{st} \tag{44}$$

where $f = 1/(T_B + T_P)$. T_P must be long enough to guarantee that V_g falls to V_{rp} in both states. If $T_P = 5T_B$, [6] shows that

$$I_p = \frac{qA_p N_{st}}{6T_B}. \tag{45}$$

Values for A_p, A_s, and N_{st} are given in Table I. Substituting these in (45) yields

$$222.2 \times 10^{-6} sec \geq T_B. \tag{46}$$

The values of T_B found at six different doping concentrations are given in Table IV where

$$T_B = \frac{T_{full} + T_{empty}}{2}. \tag{47}$$

T_B is in every case smaller than the constraining time of $222.2 \times 10^{-6}(sec)$. However T_B is so small that α in (3) may be significant. This means that during a full state at temperatures near 100°C some of the stored charge may be pumped into the substrate because the inversion layer is being removed too quickly.

TABLE IV.
THE VARIATION OF T_B WITH DOPING CONCENTRATION.
NG = 42 AND L = 1220Å.

TB_{safety} (sec)	N (cm^{-3})	T_B (sec)
-6.3528×10^{-09}	$10^{17.5}$	4.0850×10^{-7}
-9.6253×10^{-10}	$10^{17.6}$	9.5794×10^{-8}
-6.7233×10^{-11}	$10^{17.7}$	2.8069×10^{-8}
$+4.1030 \times 10^{-11}$	$10^{17.8}$	1.2280×10^{-8}
$+4.8316 \times 10^{-11}$	$10^{17.9}$	7.4580×10^{-9}
$+4.4879 \times 10^{-11}$	$10^{18.0}$	5.4757×10^{-9}

CHAPTER V

CONCLUSIONS

A. ACCURACY OF THE CALCULATIONS

The computer analysis performed has four major sources of error. The modified trapping model introduces a small amount of error at low temperatures, $> 25°C$, because it does not include thermionic field emission. Lu's model may also produce significant error at or around N^* because the grains of the resistor are not all the same size and will not all reach a fully saturated condition at the same doping concentration [7].

The second source of error is the numerical integration routine, QA05A/AD. This standard routine performs its own checks for accuracy and alerts the user to potentially faulty calculations. Since the program executed without these warnings, the results were accepted as valid.

The calculation of μ_h, the hole mobility, assumes μ_h is temperature independent. This will introduce significant error at low ($< N^*$), doping concentrations, but not at higher concentrations because the mobility becomes less sensistive to temperature at high doping concentrations. Since the interesting range of doping concentrations, those that produced a positive TB_{safety}, was $> N^*$, the error introduced will be small.

B. SUGGESTIONS FOR FURTHER WORK

The sensitivity of the resistor to temperature is a major disadvantage of the cell. However it appears that only the resistor, and not the other devices in the cell,

is the major cause of the problem. The following two suggestions for further work are made with this in mind.

First an attempt should be made to optimize the cell with respect to area and temperature operating range. An optimization procedure is given below. Second an alternative to the resistor should be found and tested in the cell. Currently, at Texas A&M University, Dr. Çilingiroğlu is exploring alternatives to the resistor.

The optimization of the cell with respect to area and temperature mentioned above should proceed in the following manner. First a state-of-the-art resistor and pump gate area should be assumed. Second T_B should be equated to $1\mu s$, which is approximately the smallest acceptable value for which α in (3) can be neglected. Then the storage gate should be specified so that it is large enough to accommodate the sensing mechanism when $V_g = V_{rp}$. The refresh voltage should then be decreased until the temperature range is acceptable. (Note that if the refresh voltage is decreased the storage gate area may need to be increased because of the sensing mechanism.) Should these specifications fail to produce a working cell the area of the pump gate may be increased. The storage well should then be readjusted to meet the previous constraint.

REFERENCES

[1] U. Çilingiroğlu, "A Two-Device Bistable Memory Circuit Without Feedback Loop," *IEEE Journal of Solid-State Circuits*, vol. SC-17, pp. 593-596, June 1982.

[2] U. Çilingiroğlu, "Bistablization of MOS/RAM Cells: the Charge-Pumping-Loop Approach," in *IEEE International Conference on Circuits and Computers*, Port Chester, New York, October 1980.

[3] U. Çilingiroğlu, "A Charge-Pumping-Loop Concept for Static MOS/RAM Cells," *IEEE Journal of Solid-State Circuits*, vol. SC-17, pp. 599-603, June 1979.

[4] U. Çilingiroğlu, Bistablilization of DRAM Cells by Charge Pumping. unpublished, Dep. Elec. Eng., Texas A&M University, Feb. 1985.

[5] J. S. Brugler and P. G. A. Jespers, "Charge Pumping in MOS Devices," *IEEE Trans. Electron Devices*, vol. ED-16, pp. 297-302, March 1969.

[6] U. Çilingiroğlu, private communications, Dep. Elec. Eng., Texas A&M University, Sept. 1985

[7] N. C. C. Lu, "Monolithic Polycrystalline-Silicon Passive Devices: Theory, Realization, and Applications," *Technical Report No. G549-1*, Electrical Engineering, Stanford University, August 1981.

[8] J. Y. W. Seto, "The Electrical Properties of Polycrystalline Silicon Films," *J. Appl. Phys.*, vol. 46, pp. 5247-5254, 1975.

[9] G. Baccarani, B. Ricco, and G. Spadini, "Transport Properties of Polycrystalline Silicon Films," *J. Appl. Phys.*, vol. 49, pp. 5565-5570, 1978.

[10] M. L. Tarng, "Carrier Transport in Oxygen-Rich Polycrystalline-Silicon Films," *J. Appl. Phys.*, vol. 49, pp. 4069-4076, 1978.

[11] S. M. Sze, *Physics of Semiconductor Devices*. New York, New York: John Wiley & Sons, 1969.

[12] C. Jacoboni, C. Canali, G. Ottaviani and A. Alberigi Quaranta, "A Review of Some Charge Transport Properties of Silicon," *Solid-St. Electron.*, vol. 20, pp. 77-89, 1977.

SUPPLEMENTAL SOURCES CONSULTED

[1] D. K. Ferry and D. R. Fannin, *Physical Electronics.* Reading, Massachusetts: Addison-Wesley Publishing Company, 1971.

[2] T. I. Kamins, "Hall Mobility in Chemically Deposited Polycrystalline Silicon," *J. Appl. Phys.*, vol. 42, pp. 4357-4365, October 1971.

[3] W. Shockley, *Electrons and Holes in Semiconductors.* New York, New York: D. Van Nostrand Company, Inc., 1950.

[4] E. S. Yang, *Fundamentals of Semiconductor Devices.* New York, New York: McGraw-Hill Book Company, 1978.

APPENDIX A

COMPUTER PROGRAMS

```
C       MAIN PROGRAM
C       NUMERICAL INTEGRATION PROGRAM
        IMPLICIT REAL*8(A-Z)
        INTEGER*4 IFLAG,LEVEL
        EXTERNAL DER
        COMMON T,VGX,PHISMIN,VG1FULL,SLOPE,NI,EG,
     C          N,PO,QT,W,ET,L,NSTAR,VB,EA,PI,KS,KSIO2,
     C          E0,ES,Q,K,H,EMASS,MH,ME,TOX,QSS,ND,
     C          VRP,VRB,AS,AP,COX,UH,SVO,NG,EF


C       CONSTANTS
        pi = 3.1415927
        Ks = 11.8
        Ksio2 = 3.9
        e0 = 8.854*(10.**-14.)
        es = 11.8 * e0
        q = 1.5*(10.**-19.)
        k = 1.38*(10.**-23)
        h = 6.625 * 10.**-34.0
        emass = 9.1 * 10.0**-31.0
        mh = 0.38*emass
        me = 0.26*emass

C       SPECIFIED CELL PARAMETERS
        Tox = 750.*10.0**-8.0
        Qss = 5.0 *10.0**10.0
        Nd  = 5.0 *10.0**14.0
        Vrp = -10.0
        Vrb =  0.0
        As = 120.0*10.0**-8.0
        Ap =  24.0*10.0**-8.0
        Cox = e0*Ksio2/Tox

        ET = -.17

C       NUMERICAL INTEGRATION PARAMETERS
        AERR = 10.0**-22.0
        RERR = .001
        LEVEL = 1

C       INTERACTIVE INPUTS
        CALL LIB$ERASE_PAGE(1,1)
        CALL LIB$SET_CURSOR(16,1)
        TYPE '('' ENTER L'')'
        ACCEPT *,L
        TYPE *,L

        IF (L.EQ.1220) THEN
                QT = 1.9*10.**12.
                NG = 42
        OPEN (UNIT=6,FILE='[JBROWN.THESIS.NOW]DATA122.',STATUS='NEW')
        OPEN (UNIT=10,FILE='[JBROWN.THESIS.NOW]I122.',STATUS='NEW')
        ELSE IF (L.EQ.420) THEN
                QT = 3.*10.**12.
                NG = 119
        OPEN (UNIT=6,FILE='[JBROWN.THESIS.NOW]DATA420.',STATUS='NEW')
        OPEN (UNIT=10,FILE='[JBROWN.THESIS.NOW]I420.',STATUS='NEW')
        ELSE IF (L.EQ.230) THEN
```

```
            QT = 3.34*10.**12.
            NG = 217
      OPEN (UNIT=6,FILE='[JBROWN.THESIS.NOW]DATA230.',STATUS='NEW')
      OPEN (UNIT=10,FILE='[JBROWN.THESIS.NOW]I230.',STATUS='NEW')
      ELSE
            TYPE *,'ERROR NO L MATCH'
      END IF
      WRITE (10,'(E13.5)'),L
      WRITE (6,'(E13.5)'),L

      TYPE '('' ENTER INCSTART'')'
      ACCEPT *,INCSTART
      TYPE *,INCSTART

      TYPE '('' ENTER INCMAX'')'
      ACCEPT *,INCMAX
      TYPE *,INCMAX

      L = L*10.**-8.
      NSTART = 10.**INCSTART
      NMAX = 10.**INCMAX
      N = NSTART
      INC = INCSTART

C     DO LOOP TO INCREMENT THE DOPING CONCENTRATION
      DO WHILE (N.LT.NMAX)
      TYPE *,N

C     CALCULATE TEMPTY AT 273 DEGREES C
      T = 273
      Eg = 1.16 - (7.02*10.0**-4.0)*(T**2.0)/(T + 1108.0)
      EA = -EG/2. + 0.08-4.3*10.**-8.*(N**(1./3.))
      uh = 47.7+(495.0-47.7)/(1.0+(N/(6.3*10.0**16.0))**.76)
      LNI = 124.3904B + 1.5*DLOG(2*PI*K*T)-Q*EG/(2.*K*T)
      NI = EXP(LNI) * (1./100.)**3.

      CALL NST
      CALL F2
      IF (N.GT.NSTAR) THEN
            CALL G1
      ELSE
            CALL G2
      END IF
      CALL QA05AD(TIME,DER,VRP,VGX,AERR,RERR,LEVEL,ERROR,IFLAG)

      IF (LEVEL.GE.4) THEN
            TYPE *,'LEVEL = ',LEVEL
      END IF

      TEMPTY = TIME

C     CALCULATE TFULL AT 373 DEGREES C
      T = 373
      Eg = 1.16 - (7.02*10.0**-4.0)*(T**2.0)/(T + 1108.0)
      EA = -EG/2. + 0.08-4.3*10.**-8.*(N**(1./3.))
      uh = 47.7+(495.0-47.7)/(1.0+(N/(6.3*10.0**16.0))**.76)
      LNI = 124.3904B + 1.5*DLOG(2*PI*K*T)-Q*EG/(2.*K*T)
      NI = EXP(LNI) * (1./100.)**3.

      CALL NST
```

```
      CALL F2
      IF (N .GT. NSTAR) THEN
            CALL G1
      ELSE
            CALL G2
      END IF
      CALL QA05AD(TIME,DER,VRP,VGX,AERR,RERR,LEVEL,ERROR,IFLAG)

      IF (LEVEL.GE.4) THEN
            TYPE *,'LEVEL = ',LEVEL
      END IF

      TFULL = TIME
      TBSAFETY = TFULL - TEMPTY
      AVE = (TFULL + TEMPTY)/2.
      TB = AVE/(1.5*10.**-8.)
      WRITE (10,'(4E13.5)'),TBSAFETY,AVE,N,TB

      INC = INC + .1
      N = 10.**INC
      END DO
      CLOSE(6)
      CLOSE(10)
      END


      FUNCTION DER(VG)
      IMPLICIT REAL*8(A-Z)
      COMMON T,VGX,PHISMIN,VG1FULL,SLOPE,N1,EG,
     C       N,PO,QT,W,ET,L,NSTAR,VB,EA,PI,KS,KSIO2,
     C       E0,ES,Q,K,H,EMASS,MH,ME,TOX,QSS,ND,
     C       VRP,VRB,AS,AP,COX,UH,SVO,NG,EF

      pc = 1.0/(uh*po*q)
      Vgrain = (Vrb - Vg)/Ng
      Vbo = Vgrain
      Vc = 0.0

      JB = 1.0
      JC = 0.0

C     ITERATIVE CALCULATION OF JB
      Do While (JC .lt. JB)
            R  = (k*T/(2.0*pi*mh))**.5
            S1 = (exp(q*Vbo/(2.0*k*T))-exp(-q*Vbo/(2.0*k*T)))/2.0
            JB = 2.0*q*po*R*exp(-q*VB/(k*T))*s1*100.0
            Vc = Vc + .001

            IF (VC .GT. VGRAIN) THEN
            VC = VGRAIN
            END IF

            Vbo = Vgrain - Vc

            ARG = L - W*2.

C           JC = 0 IF THE GRAIN IS COMPLETELY DEPLETED
            IF (ARG .EQ. 0) THEN
                  goto 7
            ELSE
```

```
                JC = Vc/((L-2.0*W)*pc)
            END IF
        end do
7       CONTINUE
        IF (JB .EQ. 0.0) THEN
            JB = Vgrain/((L-2.0*W)*pc)
            TYPE *,'JB = 0','DER'
        END IF

C       USE THE APPROPRIATE VALUE OF H DEPENDING ON THE STATE OF THE CELL
        IF (T.EQ.273) THEN
            DDER = JB/((Ap*Cox)*(1.0-slope))
        ELSE IF (VG.LT.VG1FULL) THEN
            bot = 1.0-Ap/((Ap+As)*(1.0+Svo/(2.0*(-PHISMIN)**.5)))
            DDER = JB/(Ap*Cox*bot)
        ELSE
            DDER = JB/((Ap*Cox)*(1.0-slope))
        END IF

        DER = 1.0/DDER
        RETURN
        END
```

```
      SUBROUTINE G1
C     CALCULATE PO,VB, AND W FOR N>NSTAR
      IMPLICIT REAL*8(A-Z)
      COMMON T,VGX,PHISMIN,VG1FULL,SLOPE,NI,EG
      COMMON N,PO,QT,W,ET,L,NSTAR,VB,EA,PI,KS,KS1Q2
      COMMON E0,ES,Q,K,H,EMASS,MH,ME,TOX,QSS,ND
      COMMON VRP,VRB,AS,AP,COX,UH,SVO,NG,EF

C     CALCULATE THE FERMI LEVEL
C     INITIALIZE THE DO LOOP PARAMETERS
      EF = 0.0
      ACCURACY = 1.0
      DO WHILE (ACCURACY.GT..01)
         EF = EF - .00001
         PO = (NI)*EXP(-(EF+Q)/(K*T))
         NPLUS = (N)/(1+2*EXP((EA-EF)*Q/(K*T)))
         SMALLEST = DMIN1(PO,NPLUS)
         DIF = ABS(PO-NPLUS)
         ACCURACY = DIF/SMALLEST
         IF (EF .LT. -.56) THEN
            TYPE *,'ACCURACY ON EF UNACHIEVABLE'
         END IF
      END DO

C     CALCULATE THE WIDTH OF THE DEPLETION REGION
C     INTIALIZE DO LOOP PARAMETERS
      W = L/2.
      INC = W*.001
      RIGHT = W - 1
      DO WHILE (W .GT. RIGHT)
         W = W - INC
         ARG = Q*Q*N*W*W/(2*ES*K*T)
         IF (ARG .LT. 50) THEN
      C     RIGHT = QT/((2*N)*(1+2*(NI/NPLUS)*EXP(-ET*Q/(K*T))
      C           *EXP(Q*Q*N*W*W/(2*ES*K*T))))
         END IF
      END DO

C     CHECK ACCURACY
      SMALLEST = DMIN1(W,RIGHT)
      DIF = ABS(W - RIGHT)
      ACCURACY = DIF/SMALLEST
      IF (ACCURACY.GT..01) THEN
         TYPE*,'DESIRED ACCURACY NOT OBTAINED,W',W
      END IF

C     CALCULATE VB
      VB = Q*N*W*W/(2.*ES)
      WRITE (6,'(1X,''THIS IS G1'')')
      WRITE (6,'(1X,''T = '',E13.5)'),T
      WRITE (6,'(6X,''PO '',13X,''NPLUS'',6X,''VB'',13X,''EF'')')
      WRITE (6,'(1X,4E13.5)'),PO,NPLUS,VB,EF
      WRITE (6,'(6X,''NI '',13X,''EA '',6X,''EG'',13X,''W'')')
      WRITE (6,'(1X,4E13.5)'),NI,EA,EG,W

      RETURN
      END
```

```
      SUBROUTINE G2
*     CALCULATE PO,VB, AND W FOR N<=NSTAR
      IMPLICIT REAL*8(A-Z)
      COMMON T,VGX,PHISMIN,VG1FULL,SLOPE,NI,EG,
     C       N,PO,QT,W,ET,L,NSTAR,VB,EA,PI,KS,KSIO2,
     C       E0,ES,Q,K,M,EMASS,MH,ME,TOX,QSS,ND,
     C       VRP,VRB,AS,AP,COX,UH,SVO,NG,EF

*     GRAIN IS COMPLETELY DEPLETED
      W = L/2.0

*     CALCULATE THE POTENTIAL BARRIER HEIGHT
      VB = q*N*W*W/(2.*es)

*     CALCULATE EF
      EF = et - VB + k*T/q * DLOG(.5*(QT/(L*N) - 1.0))

*     CALCULATE P(0)
      po = ni*exp(-EF*q/(k*T))
      WRITE (6,'(1X,''THIS IS G2'')')
      WRITE (6,'(1X,''T = '',E13.5)'),T
      WRITE (6,'(6X,''PO '',13X,''NPLUS'',6X,''VB'')')
      WRITE (6,'(1X,3E13.5)'),PO,PO,VB
      WRITE (6,'(6X,''NI '',13X,''EA   '',6X,''EG'')')
      WRITE (6,'(1X,3E13.5)'),NI,EA,EG
      RETURN
      END
```

```
      SUBROUTINE NST
      IMPLICIT REAL*8(A-Z)
      COMMON T,VGX,PHISMIN,VG1FULL,SLOPE,NI,EG,
     C       N,PO,QT,W,ET,L,NSTAR,VB,EA,PI,KS,KSIO2,
     C       E0,ES,Q,K,H,EMASS,MH,ME,TOX,QSS,ND,
     C       VRP,VRB,AS,AP,COX,UH,SVO,NG,EF

      LEFT = 0.0
      RIGHT = 1.0
      NSTAR = 10.**17.
      INC = 10.**14.

      DO WHILE (LEFT.LT.RIGHT)
         NSTAR = NSTAR + INC
         LEFT = Q*Q*NSTAR*L*L/(8*ES*K*T)-ET*Q/(K*T)
         RATIO = QT/(L*NSTAR)
         IF (RATIO .LE. 1) THEN
              NSTAR = QT/L
              TYPE *,'RATIO LT 1'
         ELSE
              RIGHT = DLOG(QT/L - NSTAR)-DLOG(2.*NI)
         END IF
      END DO

      SMALLEST = DMIN1(LEFT,RIGHT)
      DIF = ABS(LEFT-RIGHT)
      ACCURACY = DIF/SMALLEST

      IF (ACCURACY.LT..01) THEN
         TYPE *,'DESIRED ACCURACY NOT OBTAINED, NSTAR',NSTAR
      END IF
      TYPE *,NSTAR,T
      RETURN
      END
```

```
      SUBROUTINE F2
      IMPLICIT REAL*8(A-Z)
      DIMENSION VG(500),PHISP(500),RESIDVEC(500)
      INTEGER M
      COMMON T,VGX,PHISWIN,VG1FULL,SLOPE,NI,EG,
     C       N,PO,QT,W,ET,L,NSTAR,VB,EA,PI,KS,KSIO2,
     C       E0,ES,Q,K,H,EMASS,MH,ME,TOX,QSS,ND,
     C       VRP,VRB,AS,AP,COX,UH,SVO,NG,EF

*     THE BODY FACTOR
      sVo = (2.0**0*Ks*q*Nd)**.5 * 1.0/Cox
      Vo = sVo**2.0

*     THE SURFACE POTENTIAL FOR WHICH n = p = ni (n,p ARE SURFACE DENSITIES)
      phif = -k*T/q*(DLOG(Nd/ni))

*     THE WORK FUNCTION DIFFERENCE ASSUMING THE GATE IS DOPED INTO THE
*     CONDUCTION BAND
      phims = - Eg/2.0 - phif

*     THE FLAT-BAND VOLTAGE
      Vfb = phims - (Qss*q)/Cox

*     GATE VOLTAGE FOR WHICH PHISP = PHIF
      Vgx = Vfb + phif - sVo * (-phif)**.5

*     FIND THE MINIMUM STORAGE SURFACE POTENTIAL AT T = 0
      Qtmax = As * Cox * (-Vrp + Vfb + 2.*phif - sVo*(-2.*phif)**.5)

      c = Qtmax/(Cox*(Ap + As)) + Vrp - Vfb
      b = sVo
      a = 1.0
      x = (-b + (b**2.0 - 4*a*c)**.5)/(2.0*a)
      phismax = -(x**2.0)

      Qtmin = As * Cox * (-Vrp + Vfb + phismax - sVo*(-phismax)**.5)

      c = Qtmin/(Cox*(Ap + As)) + Vrp - Vfb
      b = sVo
      a = 1.0
      x = (-b + (b**2.0 - 4*a*c)**.5)/(2.0*a)
      phismin = -(x**2.0)

*     CALCULATE VG AT T = T1 FOR THE FULL STATE
      Vg1full = Vfb + phismin - sVo*(-phismin)**.5

*     CALCULATE H THE SLOPE
      M = 500

      If (T .lt. 323.) then
        vg(1) = -10.0
      else
        vg(1) = Vg1full
      end if

      Do j = 1,M
        phisp(j) = -(.5*(-svo + (vo - 4.0*(vg(j) - vfb))**.5))**2.
        vg(j+1) = vg(j) + (-vg(1) + vgx)/M
      end do
```

```
*       LEAST SQUARES APPROXIMATION (COURTESY DR. FLEMING)
        CALL LSQLINE (M,Vg,phisp,slope,intercept,residvec,sumsq,ierr)
        RETURN
        END
```

APPENDIX B

LETTER OF PERMISSION

IBM

International Business Machines Corporation

Thomas J. Watson Research Center
P.O. Box 218
Yorktown Heights, New York 10598
914/945-3000

Nicky Lu
#16-234

October 4, 1985

Ms. Jenny Brown
P. O. Box 13660
College Station, TX 77841

Dear Ms. Brown:

As per your request, this letter is used to give my permission for you to use figures and data which I published in my Ph.D. dissertation entitled "Monolithic Polycrystalline-Silicon Passive Devices: Theory, Realization, and Applications," Technical REport No. G549-1, Stanford University, Stanford, CA.

Best Wishes for your M.S. Thesis.

Sincerely,

Nicky Lu

VITA

Janet Kay Brown received her B.S. in Electrical Engineering in December 1983 from Texas A&M University. Her M.S. from Texas A&M University is expected in May 1986. Her permanent mailing address is

Janet Kay Brown
111 Woodacre Circle
Duncanville, Texas 75116.